Electronic Supplementary Material (ESI)

For

Unusual reaction in nitromethane solution: use of Cp*Rh moiety to form prussian blue analogues

Huirong Ma, Liangchen Liu, Yuluan Liao, Huatian Shi, Po Sun,* and Weibin Yu*

Institutes of Molecular Engineering and Applied Chemistry, Anhui University of Technology, Analysis and Testing Central Facility, Ma'anshan 243002, P. R. China.

E-mail: sunpoo@ahut.edu.cn; yuweibin@ahut.edu.cn

Contents

1. NMR spectra of 1-3.

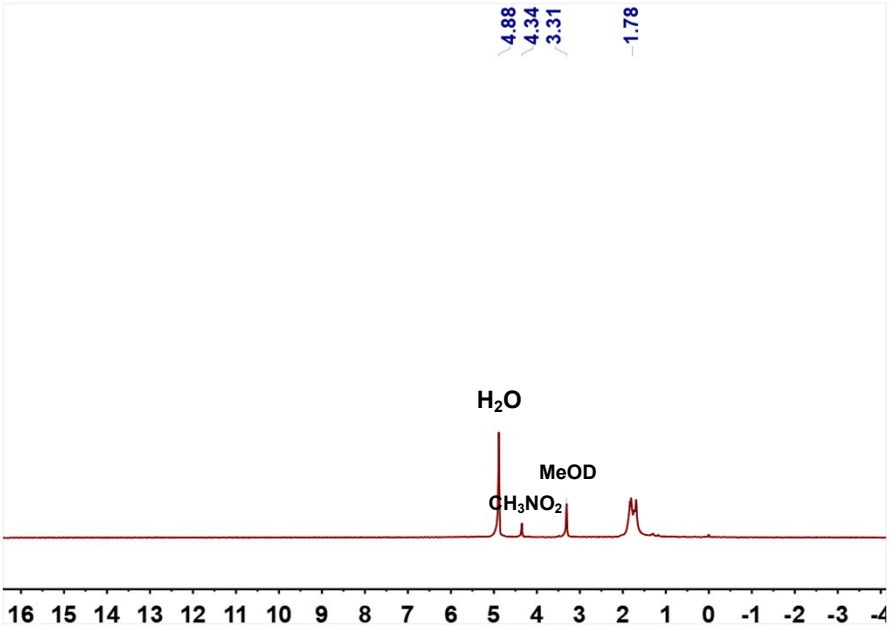

Fig. S1. ^{1}H NMR spectrum of **1** MeOD.

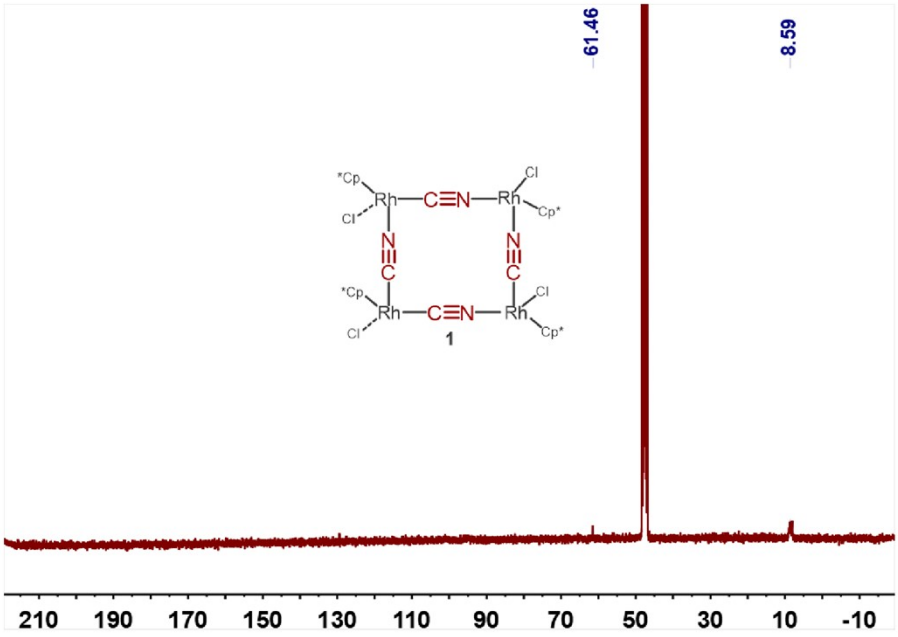

Fig. S2. ^{13}C NMR spectrum of **1** MeOD.

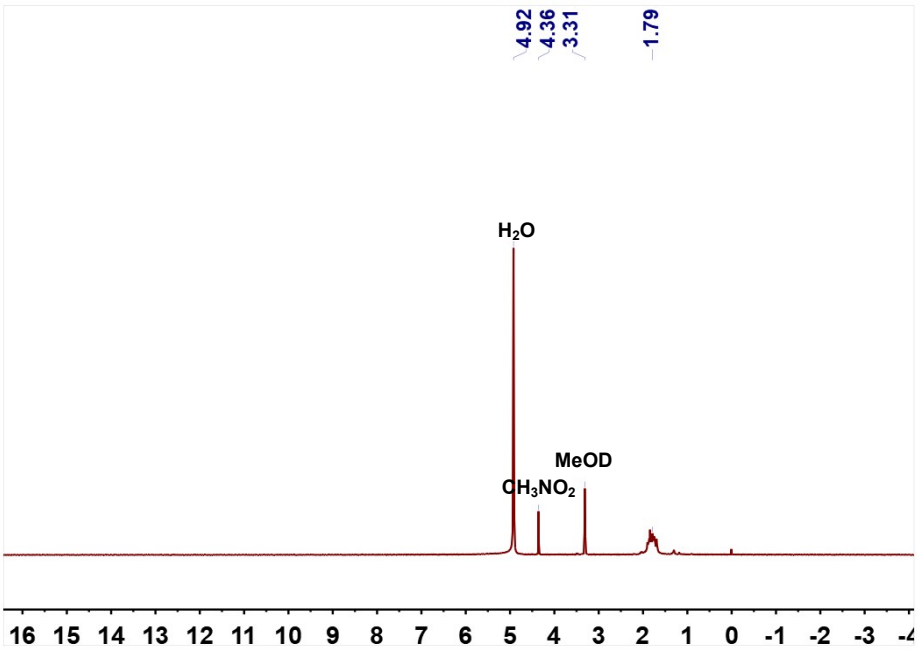

Fig. S3. ^{1}H NMR spectrum of **2** MeOD.

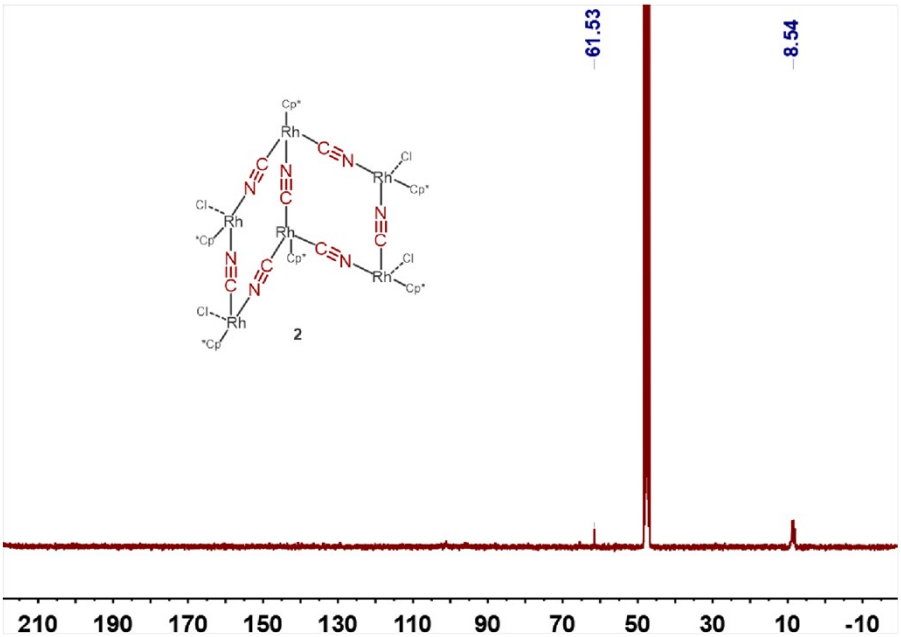

Fig. S4. ^{13}C NMR spectrum of **2** MeOD.

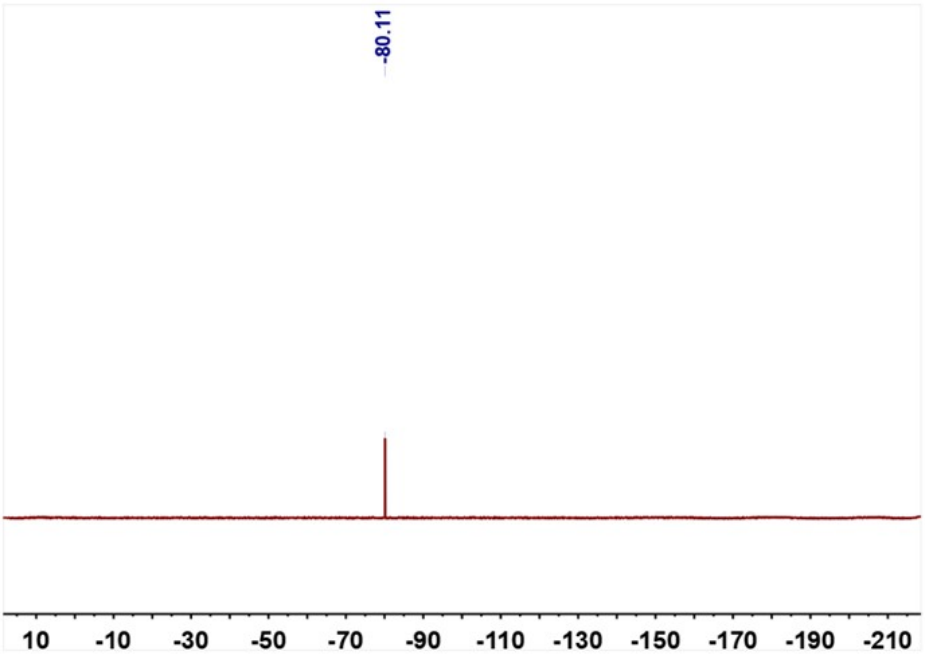

Fig. S5. ^{19}F NMR spectrum of **2** MeOD.

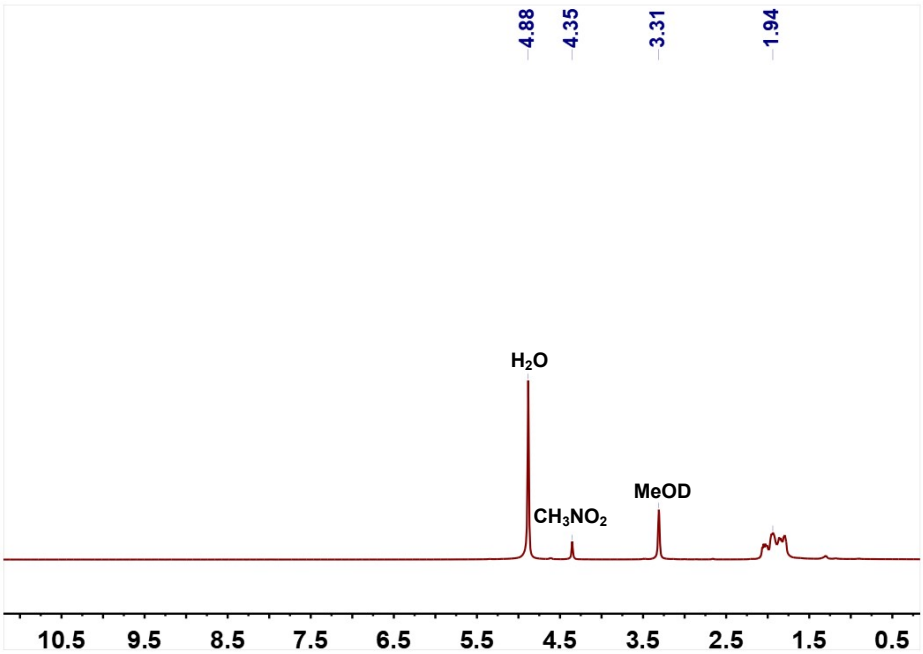

Fig. S6. ^{1}H NMR spectrum of **3** MeOD.

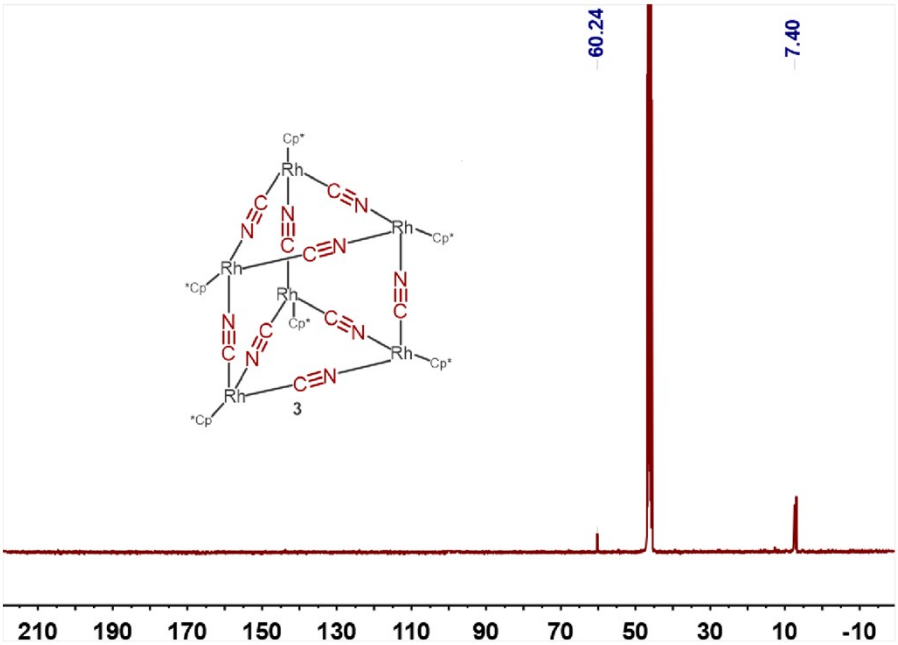

Fig. S7. ^{13}C NMR spectrum of **3** MeOD.

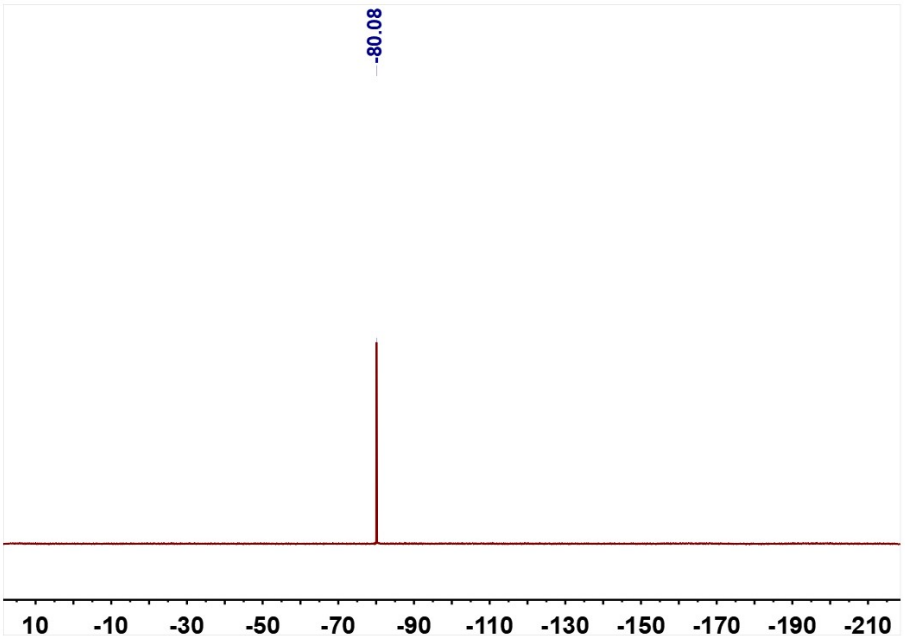

Fig. S8. ^{19}F NMR spectrum of **3** MeOD.

2. MS spectra of 1-3.

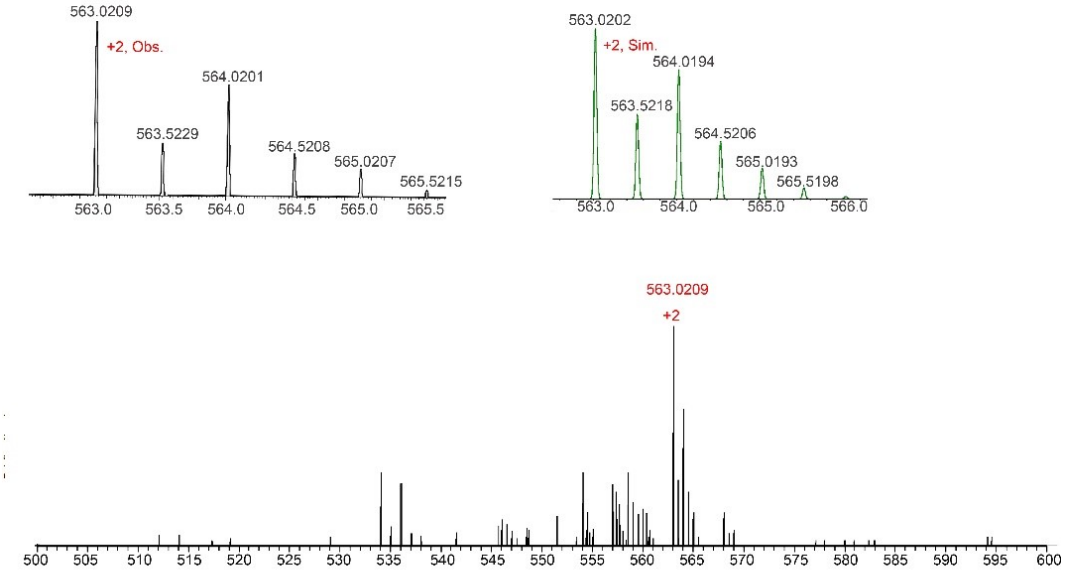

Fig. S9. The MS spectra of **1**.

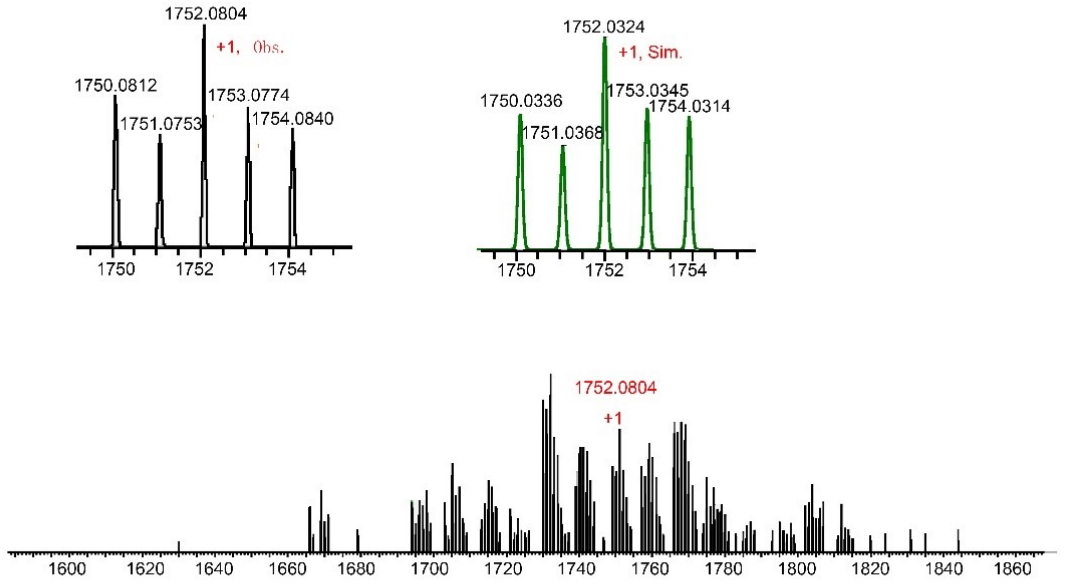

Fig. S10. The MS spectra of **2**.

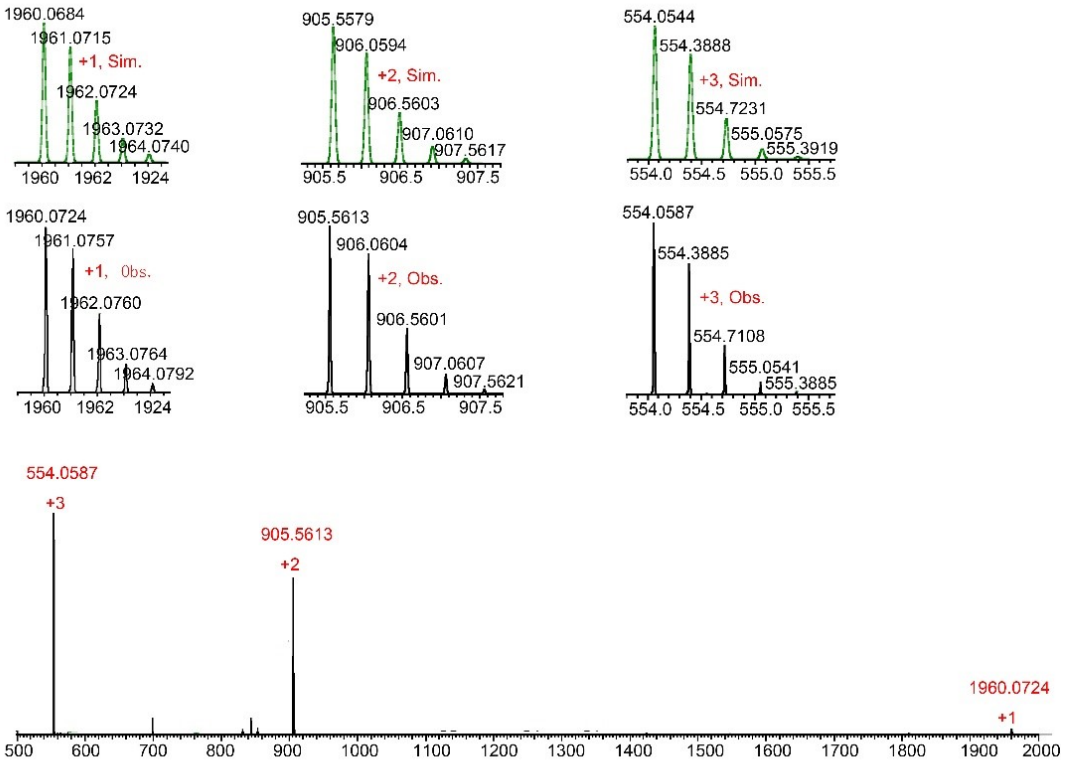

Fig. S11. The MS spectra of **3**.

3. IR spectra of 1-3.

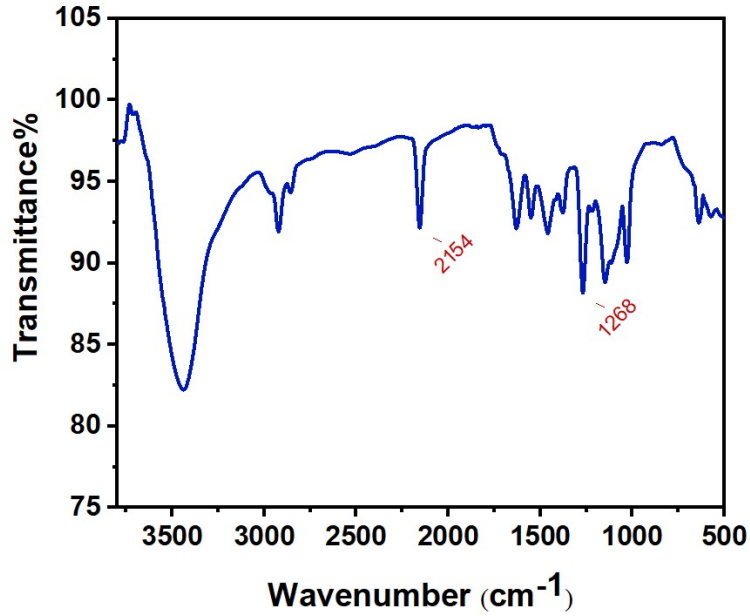

Fig. S12. IR spectra of **1**

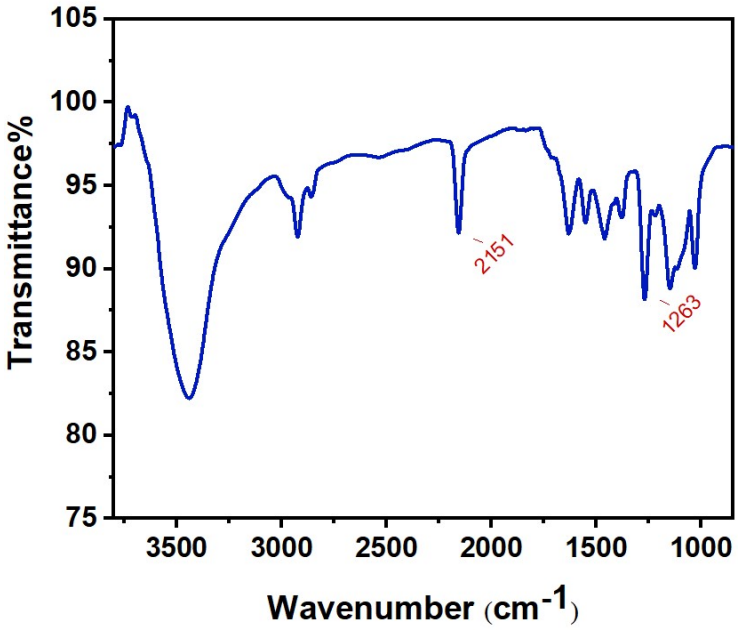

Fig. S13. IR spectra of **2**

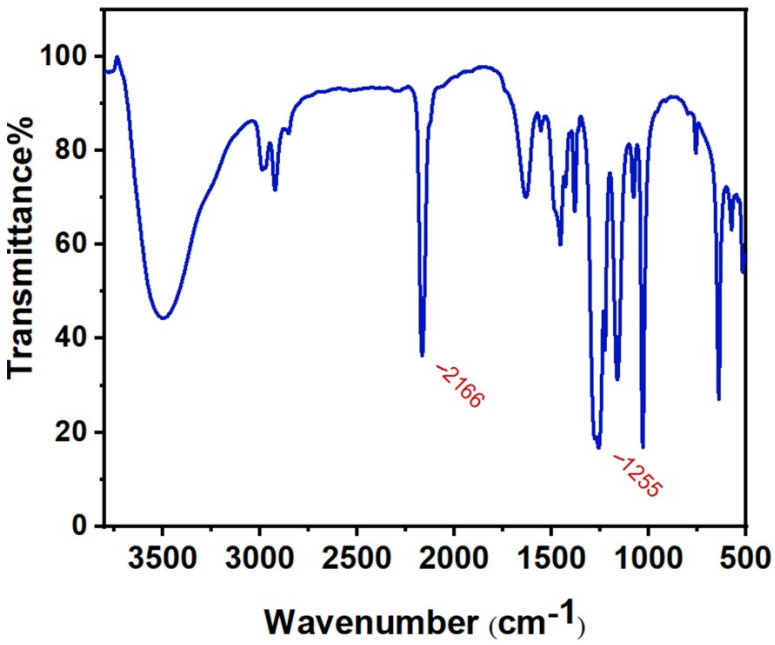

Fig. S14. IR spectra of **3**.

4. *In-situ* FTIR spectra of the reaction systems.

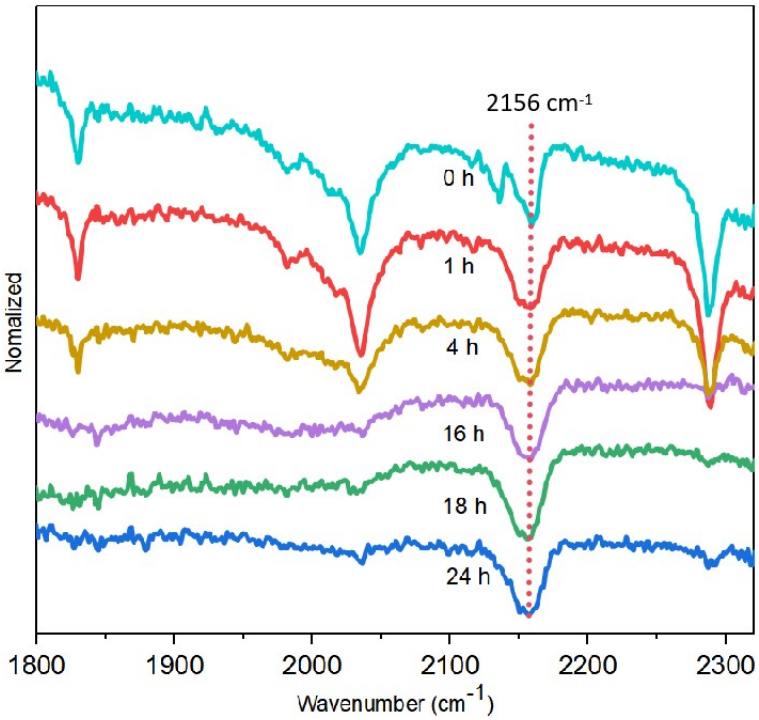

Fig. S15. In-situ FTIR spectra of the reaction system.

5. *Operando* Raman spectra.

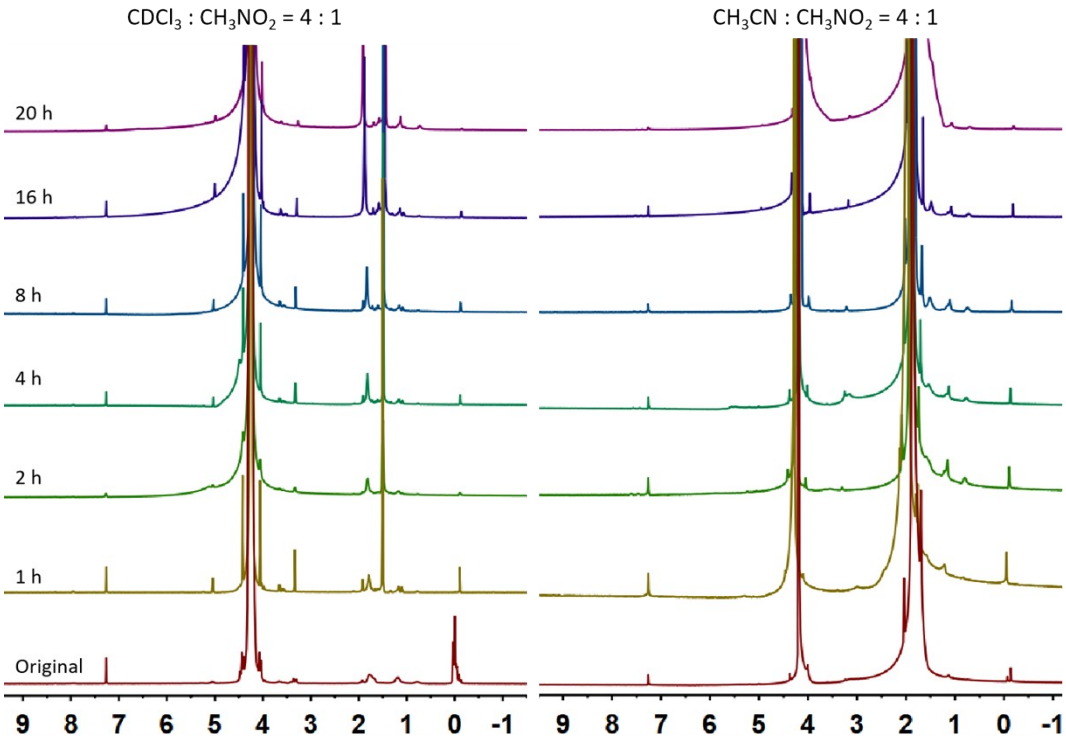

Fig.S16. ^{1}H NMR spectra were employed to monitor this reaction system.

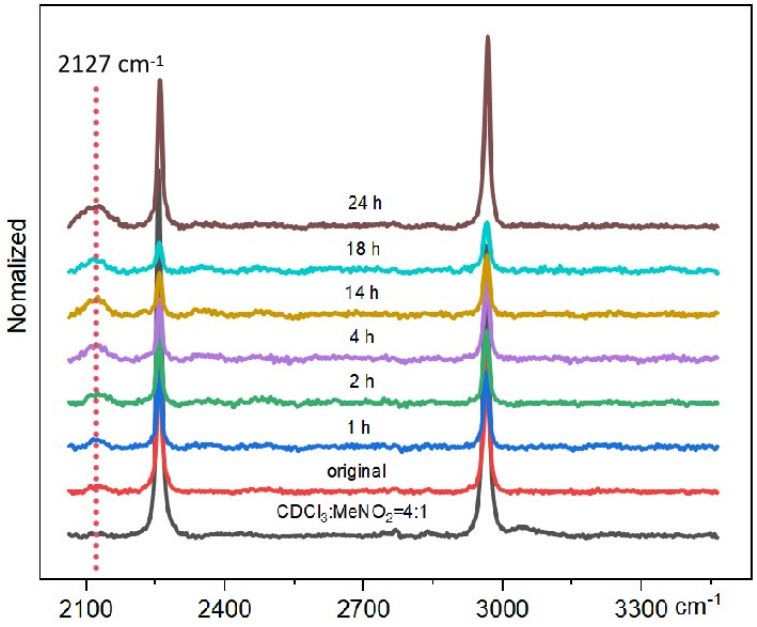

Fig. S17. Operando Raman spectra recorded on this reaction of a mount of nitromethane mixed $CDCl_3$ with $[Cp^*RhCl_2]_2$.

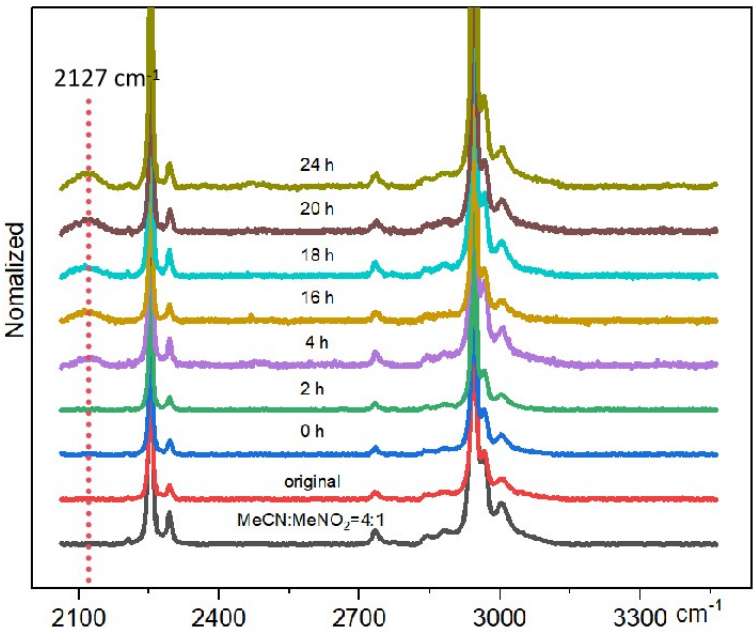

Fig. S18. Operando Raman spectra recorded on this reaction of a mount of nitromethane mixed CH_3CN with $[Cp^*RhCl_2]_2$.

6. X-ray crystal structure analysis.

Single crystals of **1-3** suitable for X-ray diffraction analysis were obtained via diffusion of diethyl ether at room temperature for several days. These crystallographic data were collected (at 296 K for **1-3**, respectively) with a Bruker D8 Venture microfocus X-ray source system. The structures was solved with the SHELXT 2018/2[1] solution program using iterative methods and by using Olex2 1.5-dev[3] as the graphical interface. The model was refined with SHELXT 2018/3[2] using full matrix least squares minimisation on F^2. In the data, the disordered solvent molecules that could not be adequately restrained were removed using the SQUEEZE routine. These data are provided free of charge by The Cambridge Crystallographic Data Centre. Additional crystallographic details can be found in **Table S1**. CCDC 2308646-2308648 (**1-3**) contain the supplementary crystallographic data for this paper.

In the crystal structure of **2**, a solvent mask was calculated and 392 electrons were found in a volume of 1750 $Å^3$ in 1 void per unit cell. This is consistent with the presence of 10[CH_3OH] per Asymmetric Unit which account for 360 electrons per unit cell.

In the crystal structure of **3**, a solvent mask was calculated and 797 electrons were found in a volume of 2955 $Å^3$ in 2 voids per unit cell. This is consistent with the presence of 11[CH_3OH] per Asymmetric Unit which account for 792 electrons per unit cell.

Table S1. Crystal data and structure refinement for **1**-**3**.

Complex	**1**	**2**	**3**
Formula	$C_{46}H_{66}Rh_4N_6O_4Cl_4$	$C_{77}H_{130}Rh_6N_7O_{10}Cl_4$	$C_{82}H_{134}F_6Rh_6N_9O_{17}S_2$
F_w	1320.48	2073.13	2313.55
cryst syst	orthorhombic	orthorhombic	monoclinic
space group	*P*bca	*P*nn2	*P* 1 21/c 1
a (Å)	16.349(4)	14.946(2)	23.390(5)
b (Å)	14.417(3)	26.441(4)	14.727(3)
c (Å)	22.659(5)	11.9783(19)	28.728(7)
α (deg)	90	90	90
β (deg)	90	90	96.413(3)
γ (deg)	90	90	90
V (Å^3)	5341(2)	4733.6(13)	9834(4)
Z	4	2	4
D_c (g.cm^{-3})	1.642	1.454	1.563
F(000)	2656	2118	4724
μ (mm^{-1})	1.460	1.186	1.101
T (K)	296	296	296
reflns/unique	26771/4706	35499/8334	22626/22626
R_{int}	0.0532	0.1017	0.1813
data/restraints/params	4706/265/300	8334/392/376	22626/1053/875
GOF on F^2	1.032	0.962	1.037
R_1, wR_2 ($I > 2\sigma(I)$)	0.0346, 0.0759	0.0563, 0.1314	0.1313, 0.2772
R_1, wR_2 (all data)	0.0532, 0.0855	0.1017, 0.1537	0.1813, 0.3047
largest diff. peak and hole (e.Å^{-3})	0.510, -0.417	0.525, -0.741	3.592, -2.929

7. References

(1) G. M. Sheldrick, *Acta Cryst.* 2015, **A71**, 3-8.

(2) G. M. Sheldrick, *Acta Cryst.* 2015, **C71**, 3- 8.